

The TOP counter and determination of bunch-crossing time at Belle II

M. Starič, for the Belle II TOP group

J. Stefan Institute, Ljubljana, Slovenia

Abstract

At the Belle II experiment a Time-of-Propagation (TOP) counter is used for particle identification in the barrel region. This novel type of particle identification device combines the Cherenkov ring imaging technique with the time-of-flight and therefore it relies on a precise knowledge of the time of collision in each triggered event. We discuss the performance of the counter and present a maximum likelihood based method for the determination of event collision time from the measured data.

Keywords: TOP counter, particle identification, collision time determination

1. Introduction

The Belle II experiment [1, 2] is a second generation of B Factory experiments aimed for the precise measurements in B , charm and τ physics as well as for the searches of physics beyond the standard model. The experiment is sited at KEK, Tsukuba, Japan. The upgraded KEKB collider, the SuperKEKB provides collisions of 4 GeV positrons with 7 GeV electrons at or near the energy of $\Upsilon(4S)$ resonance, which predominantly decays to a pair of B anti- B mesons. With similar cross-sections also pairs of $c\bar{c}$ and $\tau\bar{\tau}$ are produced, enabling to study charm and τ -lepton physics with the same collected data. The SuperKEKB collider utilizes the so called nano-beam optics, with which it is possible to squeeze the beams at the interaction region to a sub-micron dimensions and hence to achieve much larger luminosity at similar beam currents. The SuperKEKB is targeting a 30-times the luminosity of its ancestor.

The Belle II detector is a general purpose spectrometer utilizing charged particle vertexing and tracking, neutral particle detection and particle identification (PID). It consists of the following components: a vertex detector made of two layers of DEPFET sensors (PXD)¹ and four layers of double-sided silicon detectors (SVD), a central drift chamber (CDC), a time-of-propagation counter (TOP) in the barrel and a proximity focusing aerogel RICH (ARICH) in the forward, both utilizing Cherenkov ring imaging technique, a CsI(Tl) based electromagnetic calorimeter (ECL), and a K_L and muon detector system (KLM). The super-conducting solenoid coil provides a magnetic field of 1.5 T for the charged particle momentum measurements.

Except PXD all other detector components are involved in particle identification: SVD and CDC with energy loss measurements (dE/dx), TOP and ARICH exploit Cherenkov ring

imaging, ECL is involved with energy deposit measurements and KLM with penetrating power measurements. The last two components mainly contribute to lepton identification, while the first four components contribute mainly to hadron identification. All these components provide log likelihoods for the six stable or long lived charged particles: electron, muon, pion, kaon, proton and deuteron. The log likelihoods are combined by summing over detector components,

$$\log \mathcal{L}_h = \sum_{\text{det}} \log \mathcal{L}_h^{\text{det}}, \quad h = \{e, \mu, \pi, K, p, d\}. \quad (1)$$

Particle selection is performed by either using a binary PID,

$$P_{h|h'} = \frac{\mathcal{L}_h}{\mathcal{L}_h + \mathcal{L}_{h'}}, \quad (2)$$

where h and h' denote particles to be distinguished, or by a global PID,

$$P_h = \frac{\mathcal{L}_h}{\sum_{h'} \mathcal{L}_{h'}}. \quad (3)$$

It is also possible to weight the likelihoods in Eq. 3 with the corresponding prior probabilities.

The Belle II has started taking data in 2019. Since then we recorded 424 fb⁻¹, a data sample roughly equivalent to the BaBar or half of the Belle data sample, but compared to the target it represents roughly a 1% of the final goal. The luminosity has been steadily increasing during past data taking period, reaching a world record of 4.7×10^{34} cm⁻²s⁻¹ in 2022. To achieve the target of 6×10^{35} cm⁻²s⁻¹ an increase of the order of magnitude is still needed in the next years.

2. The TOP counter

The TOP counter is a variant of the DIRC detector [3]. Cherenkov photons emitted in a quartz plate by charged particles are transported to the photon detectors by means of total internal reflections. The two dimensional information about

Email address: marko.staric@ijs.si (M. Starič, for the Belle II TOP group)

¹second DEPFET layer is not completely installed yet

60 the Cherenkov ring is obtained by measuring the time-of-arrival
 61 and the position of photons at the photon detectors. The
 62 time-of-arrival is measured relative to the e^+e^- collision time
 63 and thus includes the time-of-flight of a particle. This kind
 64 of DIRC therefore combines time-of-flight measurement with
 65 Cherenkov ring imaging technique.

66 The Belle II TOP counter [4] is devoted to hadron ID in the
 67 barrel region between polar angles of 32° and 120° . It consists
 68 of sixteen modules positioned at a radius of 120 cm. The
 69 quartz optics of a module is composed of a 2.6 m long, 2 cm
 70 thick and 45 cm wide quartz plate and a 10 cm long expansion
 71 prism at backward side (Fig. 1). At forward side the quartz
 72 plate is shaped to form a spherical mirror of radius-of-curvature
 73 of 6.5 m. The prism exit window is equipped with two rows
 74 of sixteen Hamamatsu R10754 micro channel plate photo mul-
 75 tipliers (MCP-PMT) with NaKSbCs photocathode and 4×4
 76 anode readout channels [5] forming an imaging plane of 512×512
 77 pixels. These tubes are single-photon sensitive, have excellent
 78 time resolution (Fig. 2) and can work in a strong magnetic field.

79 The readout electronics is based on a 8-channel waveform
 80 sampling ASIC developed by the University of Hawaii [6].
 81 Each channel of the chip utilizes a switched-capacitor array
 82 with a sampling rate of 2.7 Gs/sec and a $11 \mu\text{s}$ long analog ring
 83 buffer for storing waveforms. Four ASIC chips are mounted on
 84 a carrier board together with a Xilinx Zynq 030-series FPGA
 85 which provides clocking and control for the ASICs. A set
 86 of four carrier boards and a data aggregator board (SCROD)
 87 equipped with a 045-series Xilinx Zynq FPGA form a front-end
 88 readout module that interfaces with the Belle II data acquisition
 89 system (DAQ). When a trigger is received, the ASIC chips dig-
 90 itize the relevant time interval of the waveforms for triggered
 91 channels using 12-bit Wilkinson-type ADC. The digitized data
 92 is then sent to the SCROD where the pedestal subtraction and
 93 feature extraction (time, amplitude and pulse width) are per-
 94 formed. The feature-extracted data are packed and sent via
 95 optical link to the DAQ system. Electronic time resolution of
 96 ~ 50 ps has been obtained for single photon signals.

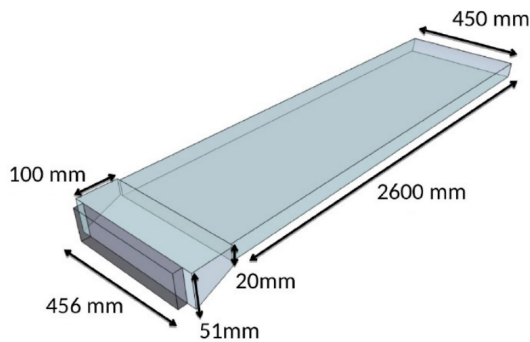


Figure 1: Quartz optics

97 3. Calibration of TOP counter

98 Calibration of TOP counter involves several steps. At first,
 99 the time base of sampling electronics of each of the 8192 elec-

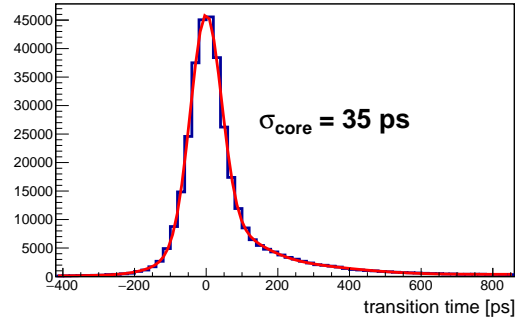


Figure 2: Transition time spread of Hamamatsu R10754.

tronic channels is calibrated with a precision better than 50 ps
 (r.m.s). This is performed by injecting double pulses of a constant
 time delay between the first and second pulse into the inputs.
 The calibration constants are determined with a minimization
 procedure described in Ref. [7]. The second step involves time
 alignment of channels within each module with a precision
 of at least 50 ps (r.m.s). This is done with a laser calibration
 system consisting of a pico-second pulsed laser source coupled
 to a light distribution system made of optical fibers and equipped
 at output with graded index micro lenses that illuminate MCP-
 PMT's uniformly as much as possible [8]. The last two steps
 are done with muons from $e^+e^- \rightarrow \mu^+\mu^-$ events, since particle
 identities are known in these events. These calibrations involve
 time alignment of modules and the calibration of bunch crossing
 time offset [7] with respect to the accelerator RF clock, with
 which the waveform-sampling electronics is synchronized; the
 precision is below 10 ps (r.m.s). Besides the timing calibrations
 we perform also masking of hot and dead channels; the masks
 are determined from the measured collision data.

The first three calibrations are found to be very stable in time.
 They are performed at the beginning of each new running period
 and cross-checked several times during that period. The bunch
 crossing time offset depends on the accelerator conditions that
 can change on a daily basis. This calibration is performed
 continuously for every run.

125 4. Particle identification with TOP counter

126 Particle identification is based on an extended likelihood
 127 method with an analytical construction of the probability density
 128 functions (PDF) [9, 10]. For a given charged particle hypothesis
 129 h ($h = e, \mu, \pi, K, p, d$) the extended likelihood is defined as
 130

$$\log \mathcal{L}_h = \sum_{i=1}^N \log \left(\frac{N_h S_h(c_i, t_i) + N_B B(c_i, t_i)}{N_h + N_B} \right) + \log P_N(N_h + N_B), \quad (4)$$

131 where N_h and $S_h(c, t)$ are the expected signal yield and signal
 132 PDF for the hypothesis h , respectively, N_B and $B(c, t)$ are the
 expected background yield and background PDF, respectively,
 and c and t are the pixel number and arrival time of the detected

135 photon, respectively. The second term in Eq. 4 is the Poisson
136 probability to measure N photons while expecting $N_h + N_B$.

137 The signal PDF for a given pixel c is parameterized as a sum
138 of m_c Gaussian PDF's:

$$S_h(c, t) = \sum_{k=1}^{m_c} n_{ck} G(t - t_{ck}; \sigma_{ck}), \quad (5)$$

139 where t_{ck} and σ_{ck} are the position and width, respectively, and
140 n_{ck} is the fraction of expected signal photons in the k -th peak.
141 Those as well as m_c are determined analytically with the model
142 described in Ref. [10]. The background PDF is modeled as
143 a uniform distribution in a time window in which the photons
144 are measured. The expected background yield N_B is estimated
145 event-by-event from the photon yields measured in other mod-
146 ules.

147 PID performance of TOP counter is governed mainly by two
148 parameters: the number of detected photons per charged par-
149 ticle and the single photon time resolution. Both have been
150 studied with collision data using muons from $e^+e^- \rightarrow \mu^+\mu^-$
151 events. The momentum range of these muons is between 4 and
152 7 GeV/c, hence the Cherenkov angle is saturated in quartz. The
153 number of detected photons per muon is measured in a time
154 window of 0 to 75 ns, the same as used for the likelihood de-
155 termination; a time window of -50 ns to 0 is taken to estimate
156 background. Background subtracted photon yields as a function
157 of muon polar angle are shown in Fig. 3. On average we
158 detect 20 to 45 photons per muon. Strong polar angle depen-
159 dence is due to several factors: muon trajectory length in the
160 quartz (proportional to $1/\sin\theta$), a fraction of Cherenkov ring
161 satisfying total internal reflection requirement, and the photon
162 losses due to light absorption, quartz surface imperfections and
163 mirror reflectivity. Photon losses are the largest for polar angles
164 around $\cos\theta \sim 0.3$ since the distance photons must travel is
165 the longest. Enhancement at nearly perpendicular muon impact
166 ($\cos\theta \sim 0$) is due to the fact that the total internal reflection
167 requirement is satisfied for the photons flying directly toward
168 PMT's (direct photons) as well as for those flying toward the
169 spherical mirror (reflected photons).

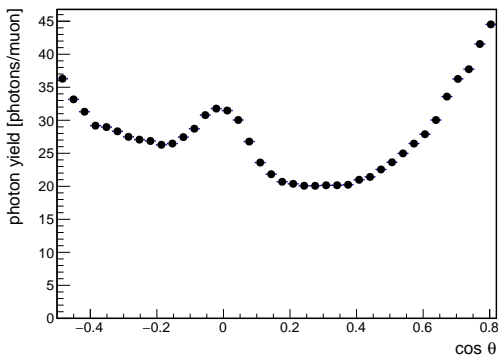


Figure 3: Number of detected photons per muon as a function of cosine of
muon polar angle.

170 With muons from $e^+e^- \rightarrow \mu^+\mu^-$ events we also measured
171 the time resolution of single photons. The main contribution

to the resolution comes from the dispersion of light in quartz
(chromatic error) and is proportional to the photon time-of-
propagation [9]. We first assigned photons to the peaks of analy-
tic PDF (Eq. 5) using sPlot technique [11]. The differences of
measured photon times and the associated peak positions were
then histogrammed in bins of photon propagation time and fi-
nally fitted with a convolution of TTS distribution (Fig. 2) and
a Gaussian distribution, whose width σ is taken as a free pa-
rameter. The results are shown in Fig. 4. A linear dependence
is clearly visible for the direct photons, while for the reflected
ones an enhanced time resolution can be noticed; this enhance-
ment is due to chromatic error corrections by focusing photons
with a spherical mirror.

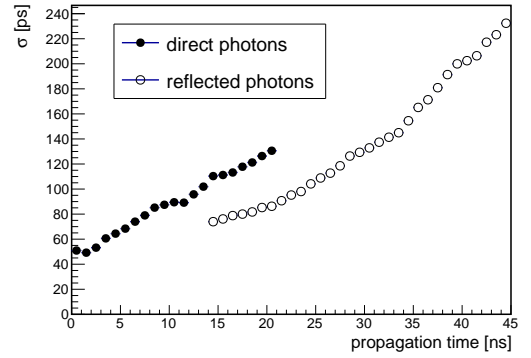


Figure 4: Single photon time resolution except TTS as a function of photon
propagation time.

Performance of kaon identification has been studied with
collision data using kinematically tagged kaons and pions
from $D^0 \rightarrow K^-\pi^+$ decays with D^0 meson reconstructed in
 $D^{*+} \rightarrow D^0\pi^+$ decay. The results for $P_{K/\pi} > 0.5$ are shown
in Fig. 5. Cherenkov threshold for kaon is at 0.5 GeV/c, while
the minimal transverse momentum needed to reach the TOP
counter is 0.27 GeV/c. Above the Cherenkov threshold and be-
low 2 GeV/c the identification efficiency is between 90% and
93% with 4% to 8% pion mis-identification (Fig. 5a). Above
2 GeV/c the performance starts to degrade; at 3 GeV/c it reaches
a broad plateau with $\sim 80\%$ efficiency and $\sim 20\%$ pion mis-
identification. Fig. 5b shows polar angle dependence. In the
backward region ($\cos\theta < 0$) the performance is better than in
the forward region primarily because of smaller particle mo-
menta. The deep in efficiency at $\cos\theta \sim 0.3$ coincides roughly
with the minimum in the photon yields shown in Fig. 3. For
these photons also the chromatic error contribution is among
the largest.

5. Determination of bunch-crossing time

The start for photon time-of-arrival measurements is given
by level one trigger whose precision (about 8 ns r.m.s.) does
not match the requirement for TOP counter (below 25 ps). This
precision can be obtained by identifying a bunch-crossing of the
collision in the off-line processing. The SuperKEKB collider
orbits bunches of particles with a frequency of 508 MHz, which

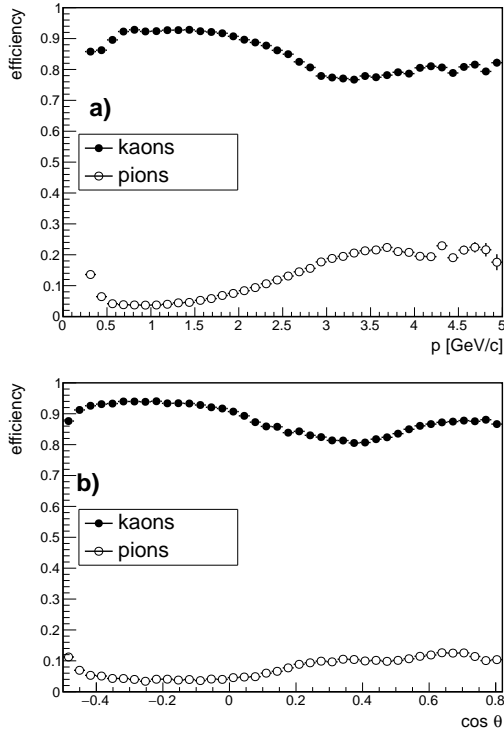


Figure 5: Kaon efficiency and pion mis-identification probability as a function of momentum (a) and cosine of polar angle (b) for $P_{K/\pi} > 0.5$ as measured with collision data using $D^{*+} \rightarrow D^0(K^-\pi^+)\pi^+$ decays.

corresponds to about 2 ns spacing between RF buckets. The length of a single bunch is 6 mm (r.m.s.), which corresponds to a 14 ps (r.m.s) spread in collision time. If the collision bunch-crossing is uniquely identified, one can correct the measured photon times by the precise timing given with the RF clock and hence can obtain the required start time precision.

The method relies on maximizing the sum of log likelihoods (Eq. 4) of particles hitting the TOP counter against a common offset subtracted from the measured photon times. At least one particle in the event that emits enough Cherenkov photons is therefore needed. Particle identities are also required; they are determined from dE/dx measurements in CDC and SVD (the most likely ones are chosen). The result of maximization is then rounded to the nearest RF bucket time and used to correct photon arrival times.

The maximum is searched by scanning a selected time interval because local maxima are usually present. This search is performed in two steps. First, a coarse scan is performed in steps of 0.5 ns within a time interval of ± 50 ns using a lookup table of time-projected PDF's. Then a fine scan is performed in a time interval of ± 5 ns around the result of the coarse scan, divided into 200 equidistant steps, and using a complete 2-dimensional PDF's. Finally, the maximum is determined precisely by fitting a parabola to the three largest values.

Efficiency of finding the correct bunch-crossing depends on particle multiplicity and is found to be very sensitive to beam background. Monte Carlo simulations of generic $B\bar{B}$ events give the following efficiencies: 98.2% if beam background is

absent, 97.4% with the present background level and 92.1% with the level expected at the SuperKEKB target luminosity. The inefficiency is found to be primarily due to false maxima caused by Cherenkov photons coming from beam background shower particles. These are not correlated with the collision time, therefore reducing the search interval should increase the efficiency. Recently, SVD can provide the collision time with ~ 1 ns precision enabling to shorten the search interval. The improved method is using the collision time determined with SVD instead of the coarse scan. In addition, falsely reconstructed bunch-crossings are suppressed by requiring reconstructed bunch-crossing to be matched with a filled bucket. With these modifications the efficiency has been largely improved: 99.9% at present background level, and 99.5% at the target luminosity where we expect a background rate of 11 MHz per PMT. The method becomes also much less dependent on particle multiplicity, as shown in Fig. 6.

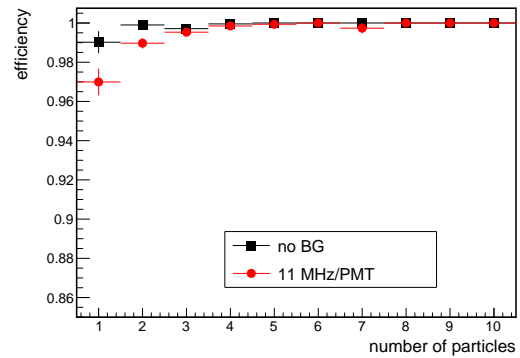


Figure 6: Efficiency of finding the correct bunch-crossing as a function of particle multiplicity. The average multiplicity of hadronic events is about 4 charged particles in the acceptance of TOP counter.

Acknowledgments

We thank the SuperKEKB group for the excellent operation of the accelerator; the KEK cryogenics group for the efficient operation of the solenoid; the KEK computer group for on-site computing support; and the raw-data centers at BNL, DESY, GridKa, IN2P3, and INFN for off-site computing support.

This work was supported by the following funding sources: European Research Council, Horizon 2020 ERC-Advanced Grant No. 884719; Slovenian Research Agency research grants No. J1-9124, J1-4358 and P1-0135.

References

- [1] <https://www.belle2.org/>
- [2] T. Abe et al., KEK Report 2010-1 (2010).
- [3] I. Adam et al., Nucl. Instr. and Meth. A 538 (2005) 281.
- [4] J. Fast, Nucl. Instr. and Meth. A 876 (2017) 145.
- [5] S. Hirose et al., Nucl. Instr. and Meth. A 787 (2015) 293.
- [6] D. Kotchetkov et al., Nucl. Instr. and Meth. A 941 (2019) 162342.
- [7] M. Starič, Nucl. Instr. and Meth. A 876 (2017) 260.
- [8] U. Tamponi, Nucl. Instr. and Meth. A 876 (2017) 59.
- [9] M. Starič et al., Nucl. Instr. and Meth. A 595 (2008) 252.
- [10] M. Starič, Nucl. Instr. and Meth. A 639 (2011) 252.
- [11] M. Pivk, F.R. Le Diberder, Nucl. Instr. and Meth. A 555 (2005) 356.